Communication

Single-Walled MoO Nanotubes

Shi Hu, and Xun Wang
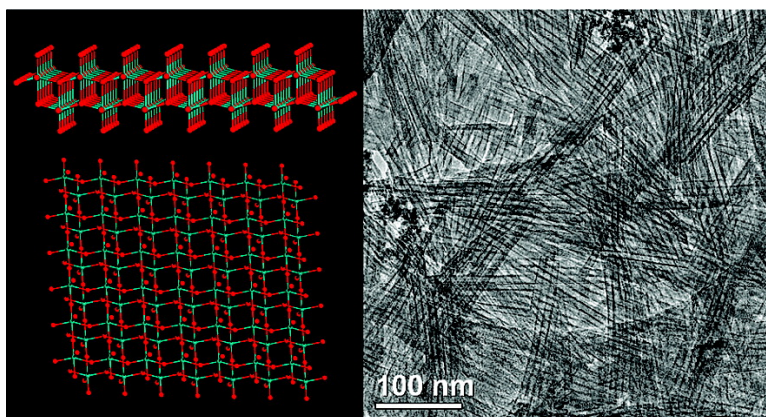
More About This Article

Additional resources and features associated with this article are available within the HTML version:

- Supporting Information
- Access to high resolution figures
- Links to articles and content related to this article
- Copyright permission to reproduce figures and/or text from this article

View the Full Text HTML

Single-Walled MoO$_3$ Nanotubes

Shi Hu and Xun Wang*

Deparment of Chemistry, Tsinghua University, Beijing, 100084, P. R. China

Received February 26, 2008; E-mail: wangxun@mail.tsinghua.edu.cn

Since the discovery of carbon nanotubes (CNT) in 1991 by Iijima,[1] tubular structured materials[2] have been greatly explored owing to their fascinating properties and potential applications.[3] Especially, single-walled carbon nanotubes (SWCNT)[4] have aroused even more extensive interests because of their intrinsic quantum effects[5] and promising advantages over their multiwalled counterparts. As compared with SWCNTs, much less success[6] has yet been achieved in the controlled growth of single-walled noncarbon nanotubes, which is impeding the extensive study and their wide applicability. Here we demonstrate the first synthesis of MoO$_3$ SWNTs via a thiol-assisted hydrothermal method.

Molybdenum trioxide (MoO$_3$) is one of the most important catalysts in modern industry. What's more, it is also a promising material in optical devices, sensors, lubricants, lithium battery, and information storage.[7] There are two basic polytypes of MoO$_3$, that is, the thermodynamically stable orthorhombic α-phase and the metastable monoclinic β-phase. The α-phase possesses a unique double-layered structure in [010] direction, each layer comprising two sublayers of corner-sharing MoO$_6$ octahedrons arranged along the [100] and [001] directions while the sublayers stack by sharing the octahedral edges along [001] (Supporting Information Figure S1). Thus, MoO$_3$ are organized with covalent bonds in plane and van der Waals forces between adjacent double-layers, which in principle makes it possible to form SWNTs. However, the rigidity endowed by these tightly bound layers makes it a real challenge to yield tubular structures as compared to other layered structures.

The controlled growth of MoO$_3$ SWNTs was based on a thiol-assisted hydrothermal method. In a typical procedure, 0.5 g of molybdic acid was used as the precursor and mixed with 25 mL of water and 5 mL of dodecanethiol. After 10 min of stirring, the mixture was sealed in an autoclave, heated to 185∼200 °C and kept for 12 h. Then the autoclave was allowed to cool naturally, and the obtained product gradually separated into two phases. The upper thiol phase was deserted, and the aquatic phase was centrifuged at 10000 rpm for 10 min. Then the turbid liquid was decanted, and the dark precipitate collected and redispersed in ethanol. Further centrifugation and dispersing of the precipitate with sonication were employed to remove most of the thiol residue, and stepwise centrifugation with increasing speed removed most of the nanoparticle impurities.

As is shown in the TEM image of Figure 1a and Supporting Information Figure 2S, large areas of cross-linked NTs lay randomly intersecting each other, along with some nanoparticle impurities. It is worth noting that all of the NTs are single-walled and have almost uniform diameters around 6 nm and a typical length of several hundred nanometers. The majority of the nanotubes are end-capped (Figure 1c inset and Supporting Information Figure S2b), and no tube-end-wrapped nanoparticles were ever observed, which may help to understand their growth mechanism. The NTs will aggregate into bundles in concentrated solution because of the high surface energy introduced by the single walls and detach into single ones after dilution and sonication, endowing them with great versatility and feasibility in basic study and device fabrication. Besides, ethanol is found to fill
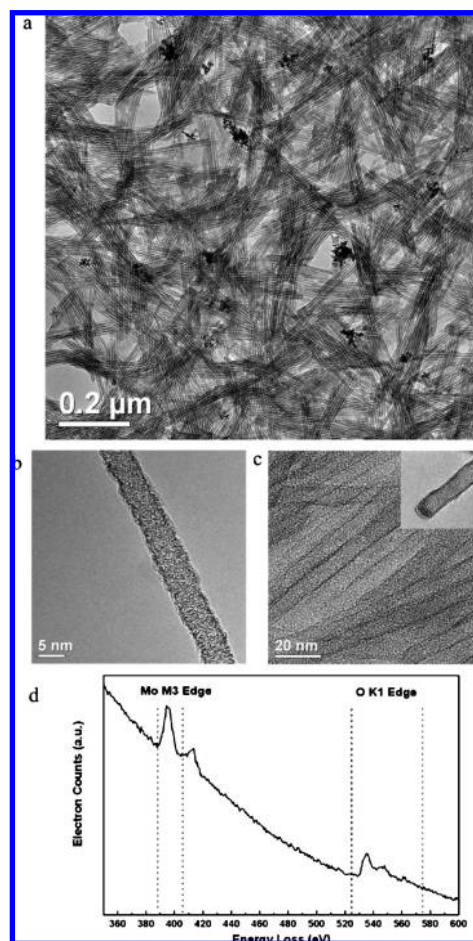

Figure 1. (a–c) Morphology of the obtained α-MoO$_3$: (a) typical TEM pictures of the cross-linked NTs on holey carbon copper grid; (b–c) local arrangement of the SWNTs in detail showing end-capping and their single-walled identity; (d) EELS spectrum of the obtained SWNTs showing Mo M3 and O K1 edge.

some open-ended tubes as segmented liquid columns which might be caused by the sonication process (indicated with arrows in Figure S2c), showing an unexplored space inside the tubes, which could be utilized. Electron energy loss spectroscopy (EELS) of the product was collected from a selected area of the grid covered with cross-linked SWNTs (Figure 1d). Apart from the carbon peaks arising from supporting film of the grid, only Mo and O peaks are recognizable from the spectrum while S is absent.[8]

As a nondestructive probe of the sample's oxidation states, X-ray photoelectron spectroscopy (XPS) measurement was conducted on the air-dried MoO$_3$ NTs cast on a silicon wafer to examine the oxidation state of Mo. Characteristic doublets of Mo 3d$_{3/2}$ at 235.3 eV and 3d$_{5/2}$ at 232.3 eV in Figure S3c show that most Mo are in the VI oxidation state, with the fact that only a small peak appears in the range of
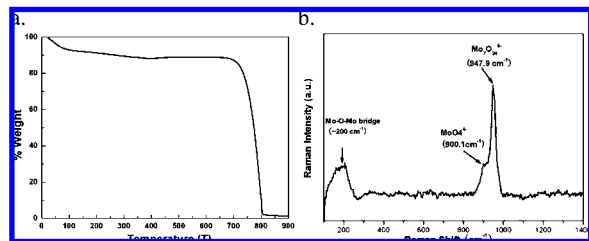
Figure 2. (a) TGA curve of the MoO₃ SWNTs with a gentle decrease under 500 °C due to the decomposition of organic impurities and a sharp drop at the sublimation temperature of MoO₃ around 700 °C. (b) Raman spectra of soluble chemical species in the final homogeneous colorless solution of the thiol-free experiment

226−230 eV which corresponds to the IV oxidation state in MoO_2, MoS_2, etc. The irregular shape of the peaks could be attributed to the high strain present in the SWNTs that causes structure relaxation. The full-range spectrum (Supporting Information Figure S5) shows that negligible sulfur is present and the peak area quantification provides Mo:O element ratio as 1:3.0, which is another direct evidence of the product's identity as MoO_3.

The TGA (thermal gravimetric analysis) curve of the product was obtained after drying it in a desiccator for 12 h (see Figure 2a). In the range between room temperature and 500 °C there is a gradual weight loss up to about 11% which can be attributed to the residual solvent, organic impurities, and water. After a plateau, the curve sharply drops to near zero at around 700 °C, which is the sublimation point of MoO_3, and finally supports our conclusion. It should be noticed from the curve that no chemical transformation into MoO_3 occurs before the sublimation. The Mo content of 55.1% given by ICP data falls within acceptable range around theoretical value of 57.9% (calculated value accounting for the organic impurities and final residue).

It is a wonder that only SWNTs appear in the product with a rather uniform diameter while in previous reports of other substances, SWNTs were always haunted by their multiwalled analogues. From the point of energy, it is obviously unfavorable for the rigid bilayer to enroll into the inner wall of a multiwalled nanotube which would be only 2 nm wide if the tube diameter is 6 nm. To reveal the mystery for the growth of the SWNTs, a control experiment was carried out by treating equal amount of MoO_3 and water hydrothermally in the absence of the thiol, and no nanotubes were obtained. On the basis of this result, it is safe to conclude that the thiols (denoted as RSH) assist the formation of SWNTs. Soluble chemical species in the final homogeneous colorless solution of the thiol-free experiment was examined by Raman spectrum (Figure 2b); peaks at 947.9 cm⁻¹ clearly show the predominance of heptamolybdate ions ($Mo_7O_{24}^{6-}$ or its partially protonated ions) while the 899.4 cm⁻¹ feature comes from MoO_4^{2-} ions. On the basis of the knowledge that Mo has an tendency to coordinate with sulfur-ending molecules, many examples of which could be found in Mo based complexes and enzymes,[9] we propose an interface-controlled self-rolling mechanism. Under appropriate temperature, the thiol molecules act on the heptamolybdate ions and caused the formation of the $(MoO_3)_n(RSH)_m$ fragments. Within this temperature range, the binding of the RSH to $(MoO_3)_n$ is loose and reversible so that combination and self-reorganization of the fragments into MoO_3 could occur with the assistance of thiols (A temperature above 200 °C will cause fierce reduction of the heptamolybdate ions by the thiol, and MoO_2 nanoparticles are formed, (Supporting Information Figure S3). Since thiol and water are immiscible, the reaction can only take place at the thiol−water interfaces so that the dimension of MoO_3 will be confined and only two-dimensional single sheets can be obtained. Finally, the MoO_3 single bilayer rolls into SWNTs to release

the strain induced by the unsaturated bonds from the edges. As the tubular structure of carbon and many other inorganic substances like WS_2 is believed to result from the rolling-up of single or multiple layers with the release of surface strain, this interface-controlled self-rolling mechanism is believed to be responsible for the formation of MoO_3 SWNTs.

Ethanol dispersion of the MoO_3 NTs was dropped onto the surface of a silicon wafer to pave a continuous film. After drying it in an oven at 80 °C, a Raman spectrum was obtained (see Supporting Information Figure S4). Four characteristic peaks could be observed from the spectrum. Bands at 951, 888, and 675/437 cm⁻¹ are assigned to the terminal oxygen stretching mode, the triply connected bridge-oxygen stretching mode, and the doubly connected bridge-oxygen stretching mode, respectively, which were detailedly studied in previous reports of vacuum-evaporated amorphous MoO_3 film, showing a long shift from values of bulky crystalline and other nanostructured MoO_3.[10] Most of the other peaks could also find their identity when compared with reported values with a reasonable shift to a different extent.

In summary, we synthesized uniform MoO_3 SWNTs with a simple hydrothermal method based on a thiol-assisted mechanism. In the light of decades-long exploration of CNTs, systematic work on the MoO_3 SWNTs needs to be carried out. We hope our endeavor could blaze a new path in the field of NT research, especially in the barely explored noncarbon SWNT areas.

Supporting Information Available: Structural model of α-MoO_3, HRTEM, and full-range XPS spectrum of the SWNTs. This material is available free of charge via the Internet at http://pubs.acs.org.

References

(1) Iijima, S. *Nature* **1991**, *354*, 56.
(2) (a) Tenne, R. *Nature* **1992**, *360*, 444. (b) Hershfinkel, M.; Gheber, L. A.; Volterra, V.; Hutchison, J. L.; Margulis, L.; Tenne, R. *J. Am. Chem. Soc.* **1994**, *116*, 1914. (c) Chopra, N. G.; Luyken, R. J.; Cherrey, K.; Crespi, V. H.; Cohen, M. L.; Louie, S. G.; Zettl, A. *Science* **1995**, *269*, 966. (d) Li, Y. D.; Wang, J. W.; Deng, Z. X.; Wu, Y. Y.; Sun, X. M.; Yu, D. P.; Yang, P. D. *J. Am. Chem. Soc.* **2001**, *123*, 9904. (e) Goldberger, J.; Fan, R.; Yang, P. D. *Acc. Chem. Res.* **2006**, *39*, 239.
(3) (a) Lu, W.; Lieber, C. M. *Nat. Mater.* **2007**, *6*, 841. (b) Deheer, W. A.; Chatelain, A.; Ugarte, D. *Science* **1995**, *270*, 1179. (c) Dai, H. J.; Hafner, J. H.; Rinzler, A. G.; Colbert, D. T.; Smalley, R. E. *Nature* **1996**, *384*, 147. (d) Kong, J.; Franklin, N. R.; Zhou, C. W.; Chapline, M. G.; Peng, S.; Cho, K. J.; Dai, H. J. *Science* **2000**, *287*, 622.
(4) (a) Bethune, D. S.; Kiang, C. H.; Vries, M. S. d.; Gorman, G.; Savoy, R.; Vazques, J.; Beyers, R. *Nature* **1993**, *363*, 605. (b) Iijima, S.; Ichihashi, T. *Nature* **1993**, *363*, 603.
(5) Bockrath, M.; Cobden, D. H.; Lu, J.; Rinzler, A. G.; Smalley, R. E.; Balents, T.; McEuen, P. L. *Nature* **1999**, *397*, 598.
(6) (a) Lee, R. S.; Cavillet, J.; Chapelle, M. L. d. l.; Loiseau, A.; Cochon, J. L.; Pigache, D.; Thibault, J.; Willaime, F. *Phys. Rev. B* **2001**, *64*, 121405. (b) Remskar, M.; Mrzel, A.; Skraba, Z.; Jesih, A.; Ceh, M.; Demsÿar, J.; Stadelmann, P.; Levy, F.; Mihailovic, D. *Science* **2001**, *292*, 479.
(7) (a) Chen, K.; Xie, S.; Bell, A. T.; Iglesia, E. *J. Catal.* **2001**, *198*, 232. (b) Bechinger, C.; Ferrere, S.; Zaban, A.; Sprague, J.; Gregg, B. A. *Nature* **1996**, *383*, 608. (c) Ferroni, M.; Guidi, V.; Martinelli, G.; Sacerdoti, M.; Nelli, P.; Sberveglieri, G. *Sens. Actuators, B* **1998**, *48*, 285. (d) Sheehan, P. E.; Lieber, C. M. *Science* **1996**, *272*, 1158. (e) Mai, L.; Hu, B.; Chen, W.; Qi, Y.; Lao, C.; Yang, R.; Dai, Y.; Wang, Z. L. *Adv. Mater.* **2007**, *19*, 3712. (f) Yao, J. N.; Hashimoto, K.; Fujishima, A. *Nature* **1992**, *355*, 624. (g) Li, X. L.; Liu, J. F.; Li, Y. D. *Appl. Phys. Lett.* **2002**, *81*, 4832.
(8) Wang, D.; Su, D. S.; Schlögl, R. *Z. Anorg. Allg. Chem.* **2004**, *630*, 1007.
(9) Li, H.; Palanca, P.; Sanz, V.; Lahoz, L. *Inorg. Chim. Acta* **1999**, *285*, 25.
(10) Ajito, K.; Nagahara, L. A.; Tryk, D. A.; Hashimoto, K.; Fujishima, A. *J. Phys. Chem.* **1995**, *99*, 16383–16388.

JA801448C